The Astrophysical Journal, 639:999–1006, 2006 March 10

GRAVITATIONAL RADIATION TIMESCALES FOR EXTREME MASS RATIO INSPIRALS

Jonathan R. Gair
Institute of Astronomy, Madingley Road, Cambridge CB3 0HA, UK

Daniel J. Kennefick
Theoretical Astrophysics, California Institute of Technology, Pasadena, CA 91125; and Department of Physics, University of Arkansas, Fayetteville, AR 72701

and

Shane L. Larson
Center for Gravitational Wave Physics, Pennsylvania State University, University Park, PA 16802
Received 2005 August 26; accepted 2005 November 7

ABSTRACT

The capture and inspiral of compact stellar objects into massive black holes is an important source of low-frequency gravitational waves (with frequencies $\sim$1–100 mHz), such as those that might be detected by the planned *Laser Interferometer Space Antenna* (*LISA*). Simulations of stellar clusters designed to study this problem typically rely on simple treatments of the black hole encounter that neglect some important features of orbits around black holes, such as the minimum radii of stable, nonplunging orbits. Incorporating an accurate representation of the orbital dynamics near a black hole has been avoided due to the large computational overhead. This paper provides new, more accurate expressions for the energy and angular momentum lost by a compact object during a parabolic encounter with a nonspinning black hole, and the subsequent inspiral lifetime. These results improve on the Keplerian expressions that are now commonly used and will allow efficient computational simulations to be performed that account for the relativistic nature of the spacetime around the central black hole in the system.

Subject headings: black hole physics — gravitational waves

1. INTRODUCTION

The event rate for detection of extreme mass ratio inspirals (EMRIs) with *LISA* depends on the efficiency of capture of compact objects by massive black holes in galactic nuclei. Current event rate estimates (Gair et al. 2004) are derived using results from stellar dynamics simulations of nuclear star clusters (Hils & Bender 1995; Sigurdsson & Rees 1997; Freitag 2001, 2003; Freitag & Benz 2002; Ivanov 2002; Hopman & Alexander 2005), in which the clusters are dynamically evolved over the lifetime of a galaxy. Of central importance to these simulations is the estimate of the effect of gravitational radiation on the evolution of a particle's orbital parameters as a function of proximity to the central black hole. The comparison of gravitational radiation timescales against cluster interaction timescales is a way to quantify whether a star stays bound to the black hole (eventually spiraling in to its death) or whether it returns to the parent star cluster and is scattered away from the black hole by encounters with other stars. Scattering by other stars can also put the star onto a quasi-radial orbit so that it plunges into the black hole directly rather than inspiraling gradually. *LISA* will only be able to detect long-lived inspirals (Gair et al. 2004), so it is important to quantify the fraction of captures that terminate in these two distinct ways. Simulations suggest that a significant fraction of captures will end in quasi-radial plunges rather than inspirals (Hils & Bender 1995; Hopman & Alexander 2005), which will impact the *LISA* event rate.

For any given encounter with the central black hole, the gravitational radiation inspiral lifetime $\tau_{\rm gw}$ of a member of the population is compared against the two-body relaxation timescale $\tau_{\rm rlx}$ with other particles in the simulation. For an orbit of eccentricity e, if $\tau_{\rm gw} < (1-e)\tau_{\rm rlx}$, the particle is removed from the simulation, and its orbital parameters are used to estimate the strength of the gravitational waves that might reach our detectors. If the relaxation timescale is such that $(1-e)\tau_{\rm rlx} < \tau_{\rm gw}$, then two-body encounters with other cluster members will alter the pericenter distance of a particle's orbit before gravitational radiation reaction causes it to merge with the central black hole (Sigurdsson & Rees 1997; Ivanov 2002).

The conventional method for treating gravitational radiation in these simulations is to use the formalism of Peters & Mathews (1963) and Peters (1964), which assumes that the particles and central masses are pointlike, Newtonian objects and that the particle orbits are Keplerian trajectories. This framework does not account for the fact that the central body is a black hole and that the orbits and orbital evolution can be decidedly non-Keplerian in nature. This paper presents an improvement to the traditional Peters & Mathews treatment, based on perturbative calculations. By exploiting the extreme mass ratio of the system, the inspiraling object can be regarded as a small perturbation of the spacetime of the central black hole. While black hole perturbation theory is well understood (Poisson 2004), the solution requires extensive numerical calculations for general orbits. However, the orbits of interest in stellar dynamics calculations are usually highly eccentric, and for such orbits the inspiral timescale can be estimated to an accuracy of $\sim$1% (depending on the precise eccentricity at capture) simply by knowing the change in eccentricity during the first encounter with the black hole.

Data for the energy and angular momentum change on a parabolic orbit are available in the literature (Martel 2004) and can be used as a starting point for treating the dynamics of EMRIs. On the basis of an understanding of the properties of geodesics in the Schwarzschild spacetime, it is possible to fit a simple function to these data; the corresponding formulae are all that are required by stellar dynamics codes and represent a significant improvement over the standard Keplerian treatment (Peters & Mathews 1963).

This paper is organized as follows. Section 2 describes geodesics in the Schwarzschild spacetime and provides fits for the total radiated energy ΔE and angular momentum ΔL on single parabolic encounters with the black hole. Section 3 presents an expression for the inspiral lifetime based on these fits. In § 4 we briefly discuss how the gravitational radiation losses from orbits of arbitrary (low) eccentricity can be estimated, and finally, § 5 summarizes the implications and possible applications of this work.

2. GEODESICS AND GRAVITATIONAL WAVE FLUXES FOR PARABOLIC ORBITS

The results of Peters & Mathews (1963) for the radiated energy and angular momentum and the inspiral lifetime are simple to implement, with a low associated computational cost. This makes them ideal for use in large simulations. The formalism has the disadvantage that it treats the binary components as point masses on Keplerian orbits. Captured stars that evolve into an EMRI generally must pass very close to the black hole, where the orbit is very non-Keplerian. The Peters & Mathews treatment neglects important features of the gravitational wave emission due to the presence of the black hole.

One simple improvement that can be made is to use a "semirelativistic" approximation, i.e., using the fully relativistic orbit in place of the Keplerian orbit, while using an approximation for the corresponding gravitational wave emission. This approach was first suggested by Ruffini & Sasaki (1981) and is explored extensively in a companion paper (Gair et al. 2005). To compute radiation fluxes correctly, one must use black hole perturbation theory and solve the Teukolsky equation (Poisson 2004). The problem of radiation from orbits in the Schwarzschild spacetime was examined by Cutler et al. (1994). They provided useful asymptotic results for nearly circular and nearly plunging orbits and tabulated fluxes for orbits with a variety of periapses and eccentricities. However, their code worked in the frequency domain, which is not well suited for dealing with the highly eccentric orbits of interest in the capture problem. More recently, results for the fluxes of radiation from parabolic orbits in Schwarzschild have become available (Martel 2004), which were computed using a time domain code. Using insight gained from studying the geodesic equations (Gair et al. 2005), it is possible to derive a simple fitting function for the energy and angular momentum emitted that matches the perturbative results to within a fraction of a percent. This function may be implemented in stellar cluster simulations as easily as the Keplerian expressions and for little additional computational cost.

The Schwarzschild geodesic equations for an equatorial orbit (without loss of generality) are

$$\left(\frac{dr}{d\tau}\right)^2 = \left(\frac{E^2}{c^2} - c^2\right) + \frac{2GM}{r}\left(1 + \frac{L_z^2}{c^2 r^2}\right) - \frac{L_z^2}{r^2}, \quad (1)$$

$$\left(\frac{d\phi}{d\tau}\right) = \frac{L_z}{r^2}, \quad (2)$$

$$\left(\frac{dt}{d\tau}\right) = \frac{E}{(c^2 - 2GM/r)}, \quad (3)$$

where τ is the proper time along the geodesic, L_z is the conserved specific angular momentum of the particle,[1] E is the conserved specific energy, and M is the mass of the central black hole. In the weak field ($r \gg GM/c^2$ or $L_z \gg GM/c$), these reduce to the usual Keplerian equations of motion, the geodesic is a conic section, and there is a well-defined periapse and eccentricity. These are related to the orbital energy and angular momentum by

$$\frac{E}{c^2} = \sqrt{1 - \frac{GM(1-e^{\rm K})}{c^2 r_p^{\rm K}}}, \quad (4)$$

$$L_z = \sqrt{(1+e^{\rm K})GMr_p^{\rm K}}. \quad (5)$$

We have used superscript "K" to denote a parameter defined in the Keplerian way. In the strong field, relativistic effects cause the orbit to deviate from Keplerian motion, and the normal notion of eccentricity—as a geometrical parameter characterizing the shape of a conic section—is not valid. However, we can still define a relativistic orbital periapse, r_p^R, as the Schwarzschild radial coordinate of the inner turning point of the motion, and we can define a relativistic eccentricity, e^R, from r_p^R and the Schwarzschild coordinate of the outer turning point of the motion (the relativistic apoapse, r_a^R), using the usual equation

$$e^R = \frac{r_a^R - r_p^R}{r_a^R + r_p^R}. \quad (6)$$

The relationship between the relativistic parameters and the orbital energy and angular momentum is

$$\frac{E}{c^2} = \sqrt{1 - \frac{GM(1-e^R)\left[(1+e^R)c^2 r_p^R - 4GM\right]}{c^2 r_p^R\left\{(1+e^R)c^2 r_p^R - \left[3 + (e^R)^2\right]GM\right\}}}, \quad (7)$$

$$L_z = \frac{(1+e^R)c\sqrt{GM}r_p^R}{\sqrt{(1+e^R)c^2 r_p^R - \left[3+(e^R)^2\right]GM}}. \quad (8)$$

It is important to note the differences between equations (7)–(8) and equations (4)–(5). In simulations of stellar clusters, the parameters of orbits that pass close to the black hole are generally computed using the Keplerian relations. However, this is not a good approximation for orbits that pass within a few Schwarzschild radii of the black hole. The energy and angular momentum are well defined out in the cluster where the orbital parameters are determined. Equating the right-hand side of equation (7) with that of equation (4), and similarly for the right-hand sides of equations (8) and (5), we can deduce a relationship between the Keplerian eccentricity and periapse and the relativistic eccentricity and periapse, for orbits that have a specified energy and angular momentum. We are mainly interested in highly eccentric orbits, so we work to linear order in $(1 - e^{\rm K})$. Thus,

$$r_p^R = \frac{r_p^{\rm K}}{2}\left(1 + \sqrt{1 - \frac{8GM}{c^2 r_p^{\rm K}}}\right) - \frac{(1-e^{\rm K})}{2}\frac{GM}{c^2}\frac{\sqrt{r_p^{\rm K}\left(r_p^{\rm K} - 8GM/c^2\right)} + r_p^{\rm K} - 8GM/c^2}{r_p^{\rm K} - 8GM/c^2},$$

$$1 - e^R = \frac{(1-e^{\rm K})}{2}\left(1 + \sqrt{1 - \frac{8GM}{c^2 r_p^{\rm K}}}\right). \quad (9)$$

[1] For equatorial orbits in Schwarzschild, the z-component of the angular momentum $L_z = L$, the total angular momentum. We maintain the notation L_z in order to facilitate future comparisons with orbits in Kerr spacetimes, for which L_z is conserved but not L.

The energy and angular momentum losses given below are expressed in terms of the relativistic (superscript "R") parameters, so it is important to use equation (9) to convert Newtonian parameters into their relativistic counterparts when evaluating gravitational wave fluxes. Indeed, even when using Peters & Mathews level approximations, one should use the relativistic rather than the Keplerian parameters for better results. This approach was used in Hopman & Alexander (2005), and we discuss it in more detail in § 4.

For the rest of this section we concentrate on parabolic orbits, i.e., orbits for which $e^{\rm K} = e^R = 1$. A parabolic orbit has $E = c^2$ and is uniquely parameterized by its periapse (or angular momentum). The angular momentum is related to the periapse by

$$L_z = \frac{\sqrt{2GM}cr_p^R}{\sqrt{c^2 r_p^R - 2GM}}. \tag{10}$$

This should be compared to the Keplerian relation, $L_z = (2GMr_p^{\rm K})^{1/2}$. The radial geodesic equation for a parabolic orbit is

$$\left(\frac{dr}{d\tau}\right)^2 = \frac{2GM}{r^3}\left(r - r_p^R\right)\left(r - \frac{2GMr_p^R}{c^2 r_p^R - 2GM}\right). \tag{11}$$

For any given eccentricity, there is a minimum value for the periapse, below which the orbit plunges directly into the black hole. This occurs when the two inner turning points of the geodesic equation coincide. For parabolic orbits this is $r_p^R = 4GM/c^2$. A geodesic with precisely this periapse asymptotically approaches a circular orbit as it nears the periapse, and it spends an infinite amount of time whirling around the black hole. The asymptotic circular orbit is an unstable orbit of the gravitational potential. Cutler et al. (1994) call this orbit the "separatrix," since it separates bound from plunging orbits in phase space.

In calculating the energy and angular momentum lost from an orbit, we must make the assumption of adiabaticity, i.e., that the timescale over which the parameters of the orbit change significantly due to gravitational radiation is much longer than the timescale of the orbit. This is valid in the extreme mass ratio limit, $m/M \ll 1$. Under this approximation, we treat the orbit as an exact geodesic of the spacetime, compute the corresponding radiation fluxes, and then update the orbital parameters to a new geodesic before repeating this procedure. A particle on a separatrix orbit would radiate an infinite amount of gravitational radiation, as it spends an infinite time "whirling" around the black hole on a nearly circular orbit. In this case, adiabaticity breaks down and it is wrong to neglect the effect of radiation reaction. In practice, a particle that starts on such an orbit would plunge into the black hole in a finite time. However, one still expects the energy and angular momentum losses to diverge as the separatrix is approached.

During the whirl phase, the orbit is almost circular, and so the total energy and angular momentum radiated will be approximately proportional to the number of "whirls" (i.e., complete revolutions in ϕ) that the orbit undergoes. Counting the number of whirls indicates that, for a parabolic orbit, the total radiated energy and angular momentum will diverge like the logarithm of $r_p^R - 4GM/c^2$ near the separatrix. The derivation of this result is given in more detail in Gair et al. (2005), and was also discussed in Cutler et al. (1994). For orbits that do not come near the black hole, the Keplerian approximation is expected to be valid. Therefore, in the limit $r_p^R \to \infty$, the energy and angular momentum radiated, ΔE and ΔL_z, should approach the Peters & Mathews results:

$$\Delta E = -\frac{85\pi}{12\sqrt{2}}c^2\frac{m}{M}\left(\frac{c^2 r_p^R}{GM}\right)^{-7/2}, \qquad \Delta L_z = -6\pi\frac{Gm}{c}\left(\frac{c^2 r_p^R}{GM}\right)^{-2}. \tag{12}$$

Our aim is to write a single expression for ΔE that can be used for any choice of r_p^R. Using the preceding arguments, we deduce that any such expression must diverge logarithmically near the separatrix at $r_p^R = 4GM/c^2$ and must recover equation (12) in the limit $r_p^R \to \infty$. Denoting $y = c^2 r_p^R/(GM)$, a functional form that has the correct behavior in these two limits is

$$\begin{aligned}\frac{M}{m}\Delta X &= F_X(y) \\ &= \left\{\sum_{n=0}^{N} A_n^X\left[\frac{(y-4)}{y^2}\right]^n\right\}\cosh^{-1}\left[1 + B_0^X\left(\frac{4}{y}\right)^{N_X-1}\frac{1}{y-4}\right] \\ &\quad + \frac{(y-4)}{y^{1+N_X/2}}\sum_{n=0}^{N} C_n^X\left[\frac{(y-4)}{y^2}\right]^n \\ &\quad + \frac{(y-4)}{y^{2+N_X/2}}\sum_{n=0}^{N-1} B_{n+1}^X\left[\frac{(y-4)}{y^2}\right]^n.\end{aligned} \tag{13}$$

In this, X is either E/c^2 or $cL_z/(GM)$ and we fix $N_E = 7$, $N_{L_z} = 4$ to give the correct leading order behavior (eq. [12]) as $r_p^R \to \infty$. The parameter N gives the order of the fit, i.e., the number of terms in the expansion that we use. To ensure that the fitting function asymptotically approaches equation (12), we impose a constraint on the coefficient C_0^X:

$$C_0^E = -\frac{85\pi}{12\sqrt{2}} - 64A_0^E\sqrt{2B_0^E}, \qquad C_0^{L_z} = -6\pi - 8A_0^{L_z}\sqrt{2B_0^{L_z}}. \tag{14}$$

Further discussion of this fitting function is given in Gair et al. (2005). In that paper, we derive the fitting function coefficients that match the results of a "semirelativistic" calculation. However, the most accurate calculation of energy and angular momentum fluxes requires solution of the Teukolsky equation. Data from such calculations are available in the literature for parabolic orbits around Schwarzschild black holes (Martel 2004). Using the data from that paper, we were able to derive fitting function coefficients to use in equation (13) that recover the Teukolsky results extremely well. In fact, taking $N = 2$ is sufficient for better than 0.2% accuracy, and the corresponding fit coefficients are

$$\begin{aligned} A_0^E &= -0.318434, \quad A_1^E = -5.08198, \quad A_2^E = -185.48, \\ B_0^E &= 0.458227, \quad B_1^E = 1645.79, \quad B_2^E = 8755.59, \\ C_0^E &= 3.77465, \quad C_1^E = -1293.27, \quad C_2^E = -2453.55, \\ A_0^{L_z} &= -2.53212, \quad A_1^{L_z} = -37.6027, \quad A_2^{L_z} = -1268.49, \\ B_0^{L_z} &= 0.671436, \quad B_1^{L_z} = 1755.51, \quad B_2^{L_z} = 9349.29, \\ C_0^{L_z} &= 4.62465, \quad C_1^{L_z} = -1351.44, \quad C_2^{L_z} = -2899.02. \end{aligned} \tag{15}$$

Figure 1 shows the percentage error in using this approximation over the range of periapse given by Martel. For comparison, we

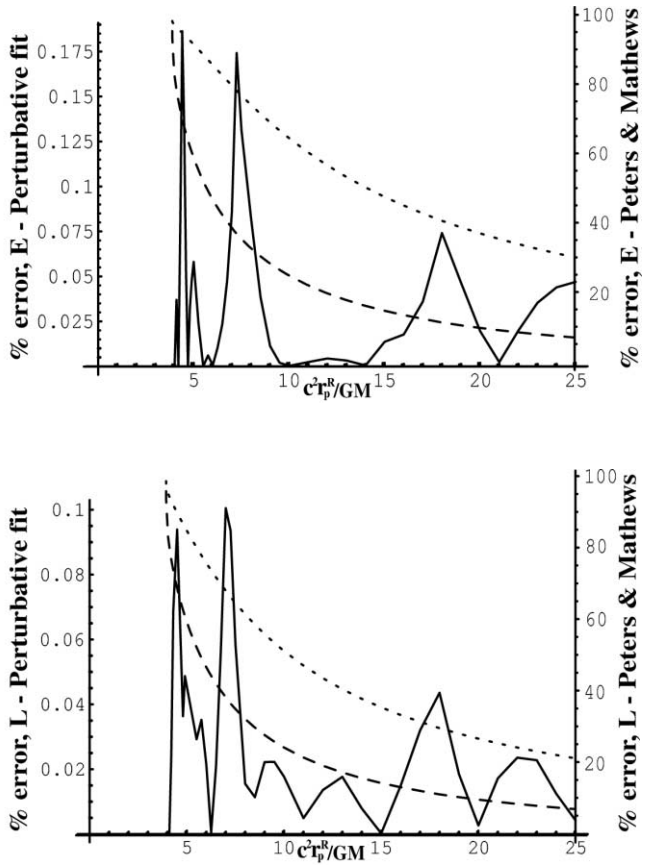

FIG. 1.—Accuracy of fit to relativistic fluxes. This figure shows the absolute percentage error when using the fitting function described in the text (*solid line*) to approximate the energy (*top*) and angular momentum (*bottom*) fluxes tabulated in Martel (2004). For comparison, we also show the error from using the Peters & Mathews result (eq. [12]), evaluated for Keplerian (superscript "K") parameters (*dotted line*) and for relativistic (superscript "*R*") parameters (*dashed line*). Two different scales have been used—the left-hand scale applies to the errors in the fitting function, while the right-hand scale applies to the errors in both applications of Peters & Mathews. The horizontal axis is the value of the relativistic periapse, $c^2 r_p^R/GM$, of the geodesic in question.

also show the error in using the Peters & Mathews result (eq. [12]), evaluated for Keplerian and relativistic parameters. The error from using the fitting function (eq. [13]) is significantly smaller than the difference between these fluxes and the Peters & Mathews results. The fluctuations in the error are due to the difference between a smooth function and noisy numerical results. The magnitude of the difference is everywhere smaller than the numerical error that Martel quotes (1%) and is a factor of approximately 1000 smaller than the error using Peters & Mathews.

Equation (13) strictly applies only to parabolic orbits, i.e., with $e^R = 1$. In realistic situations, the eccentricity at capture will be very high but less than unity, $0 < 1 - e_0^R \ll 1$. For such orbits, equation (13) can still be used and gives reliable results. The functional form fails if $r_p^R < 4GM/c^2$, but the last stable orbit (LSO) is related to the orbital eccentricity by $c^2 r_{p\mathrm{LSO}}^R = 2GM(3 + e^R)/(1 + e^R)$, and so $r_{p\mathrm{LSO}}^R > 4GM/c^2$ for all $e^R < 1$. In fact, for nonparabolic orbits, a slightly better expression for ΔE is obtained by using equation (13) with $(y - 4)$ replaced with $[y - 2(3 + e^R)/(1 + e^R)]$ and $(4/y)$ replaced with $2(3 + e^R)/[(1 + e^R)y]$ (there is some discussion of suitable fitting functions for generic orbits in Gair et al. 2005). However, for extremely eccentric orbits, this change only makes a difference for orbits that are extremely close to the LSO.

3. INSPIRAL TIMESCALES

In stellar dynamics calculations that attempt to estimate the *LISA* EMRI event rate, one must determine when a given particle is captured by the central black hole. Broadly speaking, a particle is captured when $\tau_{\mathrm{gw}} \lesssim (1 - e)\tau_{\mathrm{rlx}}$ (as before, τ_{gw} and τ_{rlx} are the timescales for gravitational wave inspiral and two-body relaxation, respectively). Heuristically, the picture is that if the orbital parameters evolve rapidly enough due to the emission of gravitational radiation, the star will spiral into the black hole (be "captured") before the cumulative perturbations to its orbit due to two-body encounters with other members of the cluster become large enough to put the star onto a new orbit, which either does not come near the central black hole or plunges directly.

The canonical estimate of τ_{gw} is given by Peters (1964) for a star that initially has semimajor axis a_0 and eccentricity e_0:

$$\tau_{\mathrm{gw}} = -\int_0^{e_0^{\mathrm{K}}} \frac{1}{de/dt}\, de = \frac{12 c_0^4}{19\beta} \int_0^{e_0^{\mathrm{K}}} de\, \frac{e^{29/19}\left[1 + (121/304)e^2\right]^{1181/2299}}{\left(1 - e^2\right)^{3/2}}, \quad (16)$$

where the constants c_0 and β are given by

$$c_0 = \frac{\left(r_p^{\mathrm{K}}\right)_0 \left(1 + e_0^{\mathrm{K}}\right)}{\left(e_0^{\mathrm{K}}\right)^{12/19}\left[1 + (121/304)\left(e_0^{\mathrm{K}}\right)^2\right]^{870/2299}}, \quad \beta = \frac{G^3}{c^5}\frac{64}{5} M^2 m. \quad (17)$$

In writing this and subsequent expressions in this section, we have assumed an extreme mass ratio, $M \gg m$ to set $M + m \approx M$.

Equation (16) is derived by integration of the Peters & Mathews fluxes over an inspiral. However, stars that become EMRI events for *LISA* are captured with very high eccentricity (typically $e \sim 0.9999$ or higher). In the limit $e_0^{\mathrm{K}} \to 1$, equation (16) becomes (Peters 1964)

$$\tau_{\mathrm{gw}}\left(r_p^{\mathrm{K}},\ e_0^{\mathrm{K}}\right) \approx \frac{24\sqrt{2}}{85} \frac{c^5}{G^3 M^2 m} \frac{\left(r_p^{\mathrm{K}}\right)^4}{\sqrt{1 - e_0^{\mathrm{K}}}}. \quad (18)$$

This form of the timescale expression is used directly in some stellar cluster simulations (Hopman & Alexander 2005) and is a very accurate approximation to the true timescale for inspirals that are initially highly eccentric. The divergence of the inspiral timescale as $e_0^{\mathrm{K}} \to 1$ arises from the divergence of the orbital timescale (at fixed periapse) in the same limit:

$$T_{\mathrm{orb}}(r_p,\ e_0) \approx \frac{2\pi}{\sqrt{GM}} \left(\frac{r_p}{1 - e_0}\right)^{3/2}. \quad (19)$$

In equation (19) (and eqs. [20] and [21] below), r_p and e can be either the relativistic or the Keplerian values, so superscripts have been omitted. Equation (19) gives the dominant piece of the timescale even accounting for the presence of the black hole. For nearly parabolic orbits

$$\frac{de}{dt} \approx \frac{\Delta e(r_p,\ e = 1)}{T_{\mathrm{orb}}(r_p,\ e)} \approx \frac{\sqrt{GM}}{2\pi} \left(\frac{1 - e}{r_p}\right)^{3/2} \Delta e(r_p,\ e = 1), \quad (20)$$

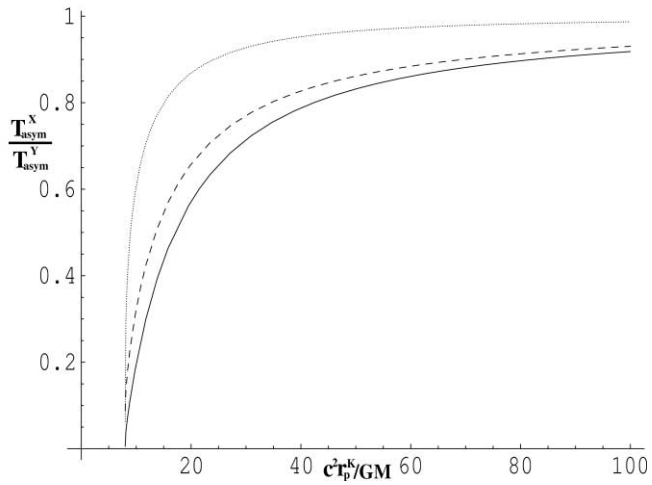

FIG. 2.—Comparison of the asymptotic approximation to the timescale in eq. (21) computed using the three methods described in the text. The plot shows the ratio $T^{\rm pert}_{\rm asym}/T^{\rm KepPM}_{\rm asym}$ (*solid line*), the ratio $T^{\rm RelPM}_{\rm asym}/T^{\rm KepPM}_{\rm asym}$ (*dashed line*), and the ratio $T^{\rm pert}_{\rm asym}/T^{\rm RelPM}_{\rm asym}$ (*dotted line*), as a function of the initial Keplerian periapse.

in which Δe is the change in eccentricity on a single orbit (the initial pass). The timescale for inspiral is dominated by

$$\tau_{\rm gw}(r_p,\ e_0) \approx -\frac{2}{\Delta e(r_p,\ e=1)}\frac{2\pi}{\sqrt{GM}}\frac{r_p^{3/2}}{\sqrt{1-e_0}}. \quad (21)$$

This expression is also given in Hopman & Alexander (2005). In the Peters & Mathews (1963) approximation,

$$\Delta e^{\rm K}\left(r_p^{\rm K},\ 1\right) = -85\pi(GM)^{3/2}Gm\Big/\left[6\sqrt{2}c^5\left(r_p^{\rm K}\right)^{5/2}\right],$$

giving the result in equation (18). Using the fits to the perturbative results, $\Delta e^R(r_p^R,\ e^R=1)$ may be expressed

$$\begin{aligned}\Delta e^R\left(r_p^R,\ e^R=1\right) &= \frac{\partial e^R}{\partial E}\Delta E\left(r_p^R,\ e^R=1\right)+\frac{\partial e^R}{\partial L_z}\Delta L_z\left(r_p^R,\ e^R=1\right)\\ &= 2\frac{r_p^R}{GM}\Delta E\left(r_p^R,\ e^R=1\right)\\ &= 2\frac{c^2r_p^R}{GM}\frac{m}{M}F_E\left(\frac{c^2r_p^R}{GM}\right), \end{aligned} \quad (22)$$

where the function $F_E(y)$ is the fit to the energy loss derived above (eqs. [13]–[15]). Together, equations (21) and (22) constitute an improved estimate of the inspiral lifetime.

Figure 2 compares the asymptotic timescale (eq. [21]) computed using three methods: $T^{\rm pert}_{\rm asym}$, generated using the perturbative result (eq. [22]); $T^{\rm KepPM}_{\rm asym}$, generated using the Peters & Mathews result (eq. [18]) evaluated for Keplerian ("K") parameters; and $T^{\rm RelPM}_{\rm asym}$, generated using the Peters & Mathews result (eq. [18]) evaluated for relativistic ("R") parameters. The figure shows the ratio of these various timescales as a function of the initial periapse of the orbit. This periapse is the *Keplerian* periapse of the orbit, which is the quantity normally evaluated in stellar cluster simulations. The Keplerian Peters & Mathews timescale is then given directly by equation (18), while the other timescales are given by first computing the corresponding relativistic periapse and eccentricity (eq. [9]). The curves are actually eccentricity dependent, but curves for different eccentricities are almost indistinguishable for the eccentricities of interest, $10^{-2} \lesssim 1-e^R \lesssim 10^{-6}$. The figure indicates that all three approximations agree for large initial periapses but deviate as the periapse is reduced. Comparing to the standard Keplerian timescale, $T^{\rm KepPM}_{\rm asym}$, for $r_p^{\rm K} \lesssim 80GM/c^2$, the perturbative timescale is smaller by 10% or more, while for $r_p^{\rm K} \lesssim 16GM/c^2$, it is more than 50% lower. This is a reasonably large discrepancy, and it therefore seems plausible that inclusion of the more accurate decay timescale in stellar cluster simulations could enhance the capture rate. On a note of caution, a parabolic Keplerian orbit with periapse $r_p^{\rm K} = 8GM/c^2$ corresponds to the relativistic orbit with periapse $r_p^R = 4GM/c^2$, i.e., the separatrix orbit. Thus, all orbits with Keplerian periapse less than $8GM/c^2$ are plunging orbits. The standard cutoff used in most stellar cluster simulations is at a Keplerian periapse of $2GM/c^2$. This correction will thus tend to *decrease* the number of capture orbits. Whether this dominates over the enhanced rate due to the reduction in inspiral lifetime is not clear, but can be determined by simulation. This is currently being pursued.

It is also clear from Figure 2 that a significant part of the improvement derives from the coordinate choice, i.e., using the relativistic periapse and eccentricity (9). A significantly improved estimate of both the radiation fluxes and the inspiral timescale can be obtained simply by evaluating the standard Peters & Mathews results (eqs. [12] and [18]) for the relativistically defined periapse and eccentricity (eq. [9]). This is discussed briefly in § 4 and in more detail in Gair et al. (2005). Nonetheless, the perturbative timescale is still more than 20% shorter for $r_p^{\rm K} \lesssim 16GM/c^2$ and should be used if possible. In Hopman & Alexander (2005), relativistic parameters are used to describe the orbit, and the cutoff for plunging orbits is correctly defined. This might explain some of the reduction in event rate that they observe, although this reduction is dominated by diffusion onto plunging orbits. Inclusion of the perturbative results described here in the same type of simulation used in Hopman & Alexander (2005) should lead to an enhancement in rate, but it is not entirely clear how large an effect this will be.

An important point to note is that both equation (21) and the Peters expression (eq. [18]) are derived by integrating the orbital averaged fluxes, $\langle de/dt\rangle$ and $\langle dr_p/dt\rangle$. In the test particle (zero mass) limit this is correct, but for nonzero mass ratios it will not be entirely accurate. The discrepancy is apparent from the fact that the gravitational decay timescale diverges like $(1-e^R)^{-1/2}$ as $e^R \to 1$, which is less rapid than the divergence of the orbital period, $(1-e^R)^{-3/2}$. If the particle was initially at periapse, the decay timescale is not too inaccurate, but in practice the particle will start near apoapse, out in the stellar cluster. Physically, there are no significant gravitational radiation losses until the particle gets close to the black hole, so the decay timescale must be at least as long as half the first orbital period. The discreteness of the GW emission should become important when one minus the initial eccentricity of the orbit, $1-e_0^R$, is less than the change in eccentricity on the first pass, $\Delta e^R(r_p^R,\ e^R=1)$, i.e., when

$$\left(1-e_0^R\right) \lesssim -2\frac{m}{M}\frac{c^2r_p^R}{GM}F_E\left(\frac{c^2r_p^R}{GM}\right). \quad (23)$$

For this eccentricity, the change in $(1-e^R)$ over the first orbit is of the same magnitude as $(1-e_0^R)$; thus, the underlying assumption that the particle completes an entire orbit on the initial

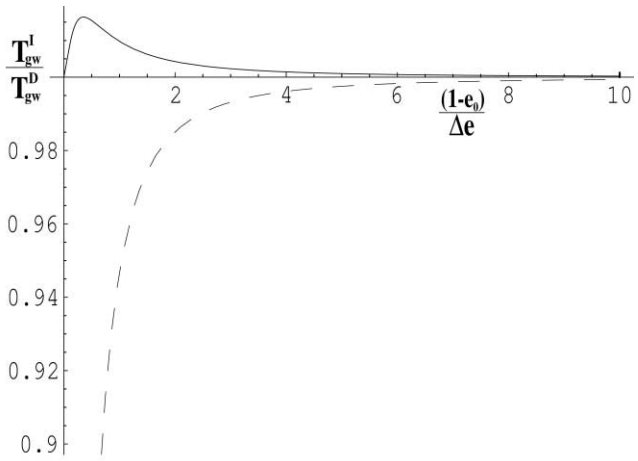

FIG. 3.—Ratio of the integral inspiral timescale (eq. [21]), $T^I_{\rm gw}$, to the discrete inspiral timescale (eq. [24]), $T^D_{\rm gw}$, as a function of $(1 - e_0^R)/\Delta e(r_p^R,\ e^R = 1)$. The dashed line uses the integral timescale computed directly from eq. (21), while the solid line includes the first half-period correction (eq. [25]).

geodesic is false. This is also the point at which the decay timescale (eq. [21]) becomes comparable to the initial orbital period, so it is clear that the assumptions are breaking down. In this regime, the gravitational wave decay timescale is more accurately computed by assuming the periapse and eccentricity change discretely at periapse, and adding up the orbital periods of this sequence of geodesics. At the same level of approximation used to derive equation (21), the corresponding GW inspiral timescale is given by

$$\tau_{\rm gw}\left(r_p^R,\ e_0^R\right) \approx \frac{\pi}{\sqrt{GM}}\left(\frac{r_p^R}{1-e_0^R}\right)^{3/2} + \frac{2\pi\left(r_p^R\right)^{3/2}}{\sqrt{GM}}\sum_{l=1}^{\infty}\frac{1}{1-e_0^R+l\Delta e^R\left(r_p^R,\ e^R=1\right)} = \frac{\pi\left(r_p^R\right)^{3/2}}{\sqrt{GM}}\left\{\left(\frac{1}{1-e_0^R}\right)^{3/2}+\left[\frac{1}{\Delta e^R(r_p^R,\ e^R=1)}\right]^{3/2} \times \zeta\left(\frac{3}{2},\ \frac{1-e_0^R}{\Delta e^R\left(r_p^R,\ e^R=1\right)}\right)\right\} \quad (24)$$

where $\zeta(z, q)$ is the generalized Riemann zeta function. The first term in equation (24) is the time taken to reach periapse from apoapse on the first pass, while the second term is the summation of orbital periods over the subsequent sequence of geodesics. This expression neglects the change in periapse on each pass, the difference in Δe^R on each pass due to the evolution of e^R and approximates a finite series (which terminates when $1 - e_0^R + l\Delta e^R$ equals the plunge eccentricity) with an infinite sum. However, these are all lower order corrections in the mass ratio, m/M, and may be neglected for initially highly eccentric EMRIs.

In the limit $1 \gg 1 - e_0^R \gg \Delta e^R(r_p^R,\ e^R = 1)$, equation (24) is equivalent to equation (21), but when $1 - e_0 \approx \Delta e^R(r_p^R,\ e^R = 1)$, this is no longer true. Figure 3 shows the ratio of the integral timescale (eq. [21]) to the discrete timescale (eq. [24]) as a function of $(1 - e_0^R)/\Delta e^R(r_p^R,\ e^R = 1)$. As expected, the integral form (eq. [21]) does well until the estimated point of breakdown (eq. [23]), but significantly underestimates the decay timescale in the extreme parabolic limit. In this regime, a more accurate orbital decay timescale can be obtained by considering the sum of half the initial orbital period plus the decay time (eq. [21]) evaluated for the orbit with periapse $r_p^{R\prime} = r_p^R + \delta r_p^R/2$ and eccentricity $e^{R\prime} = e^R + \delta e^R/2$, where δr_p^R and δe^R are the predicted change in periapse and eccentricity for the initial geodesic. In other words, we compute the integral decay timescale starting when the particle reaches periapse for the first time. This gives

$$\tau_{\rm gw}\left(r_p^R,\ e_0^R\right) = \frac{\pi}{\sqrt{GM}}\left(\frac{r_p^R}{1-e_0^R}\right)^{3/2} - \frac{M}{m}\frac{2\pi\sqrt{GM}}{c^2F_E\left[\left(c^2r_p^{R\prime}/GM\right)\right]}\sqrt{\frac{r_p^{R\prime}}{1-e^{R\prime}}}$$

$$e^{R\prime} = e^R + \frac{m}{M}\frac{c^2r_p^R}{GM}F_E\left(\frac{c^2r_p^R}{GM}\right)$$

$$r_p^{R\prime} = r_p^R + \frac{m}{M}\left[\frac{\sqrt{GM}\left(c^2r_p^R-2GM\right)^{3/2}}{\sqrt{2}c^2\left(c^2r_p^R-4GM\right)}F_{L_z}\left(\frac{c^2r_p^R}{GM}\right) - \frac{\left(r_p^R\right)^2c^2\left(c^2r_p^R-2GM\right)}{2GM\left(c^2r_p^R-4GM\right)}F_E\left(\frac{c^2r_p^R}{GM}\right)\right]. \quad (25)$$

Figure 3 also shows the ratio of the revised timescale (eq. [25]) to the discrete timescale (eq. [24]) (with the approximation $r_p^{R\prime} = r_p^R$). This expression performs very well in all regimes and is at most a 2% overestimate near $1 - e_0 = \Delta e(r_p^R,\ e^R = 1)/4$. In most situations the difference between equations (21) and (25) is small, but for any initial eccentricity, there is a mass ratio for which condition (23) holds, and in that regime equation (25) must be used. However, this expression is equally easy to evaluate in numerical codes.

4. EXTENSION TO GENERIC ORBITS

This paper has focused on parabolic orbits, as these are of most relevance for astrophysical captures. For orbits of moderate eccentricity, this analysis will break down. If data based on perturbative calculations were available for the energy and angular momentum losses on generic orbits, it would be possible to compute a fit analogous to equation (13) that could be used generically (see discussion in Gair et al. 2005). This is not true at present. However, a significantly better approximation to the fluxes can be obtained simply by evaluating the Peters & Mathews fluxes, using the relativistic (rather than the Keplerian) definition of the orbital parameters. This approach was used in Hopman & Alexander (2005).

Inversion of equations (7)–(8) yields a quadratic to give e^R and r_p^R as functions of E and L_z (which can be obtained from the Keplerian parameters using eqs. [7]–[8] if necessary). For orbits of moderate eccentricity, $e \lesssim 0.9$, it is not appropriate to use the (eccentricity-independent) flux expressions or timescale formula quoted earlier, since these were evaluated in the high-eccentricity limit. However, if the relativistic eccentricity and periapse are computed for the orbit in question, a good approximation

to the energy and angular momentum radiated can then be obtained using the Peters & Mathews expressions

$$\Delta E = -\frac{64\pi c^2}{5}\frac{m}{M}\frac{1}{(1+e^R)^{7/2}} \times \left[1+\frac{73}{24}\left(e^R\right)^2+\frac{37}{96}\left(e^R\right)^4\right]\left(\frac{c^2 r_p^R}{GM}\right)^{-7/2} \quad (26)$$

$$\Delta L_z = -\frac{64\pi}{5}\frac{Gm}{c}\frac{1}{(1+e^R)^2}\left[1+\frac{7}{8}\left(e^R\right)^2\right]\left(\frac{c^2 r_p^R}{GM}\right)^{-2}. \quad (27)$$

The corresponding inspiral timescale can be computed by integrating these fluxes along an inspiral trajectory, as in equation (16). We emphasize that for most situations of astrophysical interest in the capture problem, the parabolic results given earlier in this paper should be used. However, if fluxes for moderate eccentricity orbits are required, equations (26) and (27) evaluated for the relativistic orbital parameters perform much better in the strong field than if they are evaluated for the Keplerian orbital parameters (Gair et al. 2005). That this approach will yield a better estimate of the energy and angular momentum fluxes is not clear a priori, but has been verified by comparison with fluxes computed using perturbation theory (Gair et al. 2005). This technique essentially identifies orbits that are geometrically similar. In the strong field, a Schwarzschild geodesic with a given energy and angular momentum is nothing like the Keplerian orbit with parameters ($e^{\rm K}$, $r_p^{\rm K}$), but it does look somewhat like a Keplerian orbit with parameters (e^R, r_p^R); e.g., the turning points of the motion are at the same radii. The orbital geometry is very important for determining the radiation field, and this is probably the reason that a better estimate of the flux can be obtained via this procedure.

If more accurate fluxes are required for generic orbits, one can use the expressions quoted in Barack & Cutler (2004). These are based on post-Newtonian expansions and are therefore only approximations to the true fluxes, but improve slightly on equations (26) and (27). For parabolic orbits, the fit presented here (eqs. [13]–[15]) gives the correct energy and angular momentum flux from an extreme mass ratio orbit under the assumption of adiabaticity. It is therefore more accurate than any post-Newtonian calculation for parabolic and highly eccentric orbits, and so should be used under those circumstances. Further flux expressions are given in Gair & Glampedakis (2005), which combine fits to perturbative calculations for the fluxes from circular orbits with post-Newtonian expressions for the fluxes from eccentric orbits. The resulting expressions improve on Barack & Cutler (2004) and could be combined with equations (13)–(15) to interpolate the evolution of generic inspirals.

5. DISCUSSION

In this paper, we have presented new simple analytic expressions for the energy and angular momentum radiated in gravitational waves by and subsequent inspiral lifetime of stars that pass close to black holes on nearly parabolic orbits. These expressions are based on the results of numerical perturbative calculations that are available in the literature (Martel 2004) and are considerably more accurate than the standard Keplerian results of Peters & Mathews (1963) that are commonly used. We find that the inspiral lifetime can be significantly reduced when the capture problem is treated more carefully, which suggests an increase in the capture rate compared to the results of current simulations. However, the use of relativistic parameters for describing the orbit might actually lead to a reduction in events, since there are more plunging orbits.

Standard stellar cluster simulations (Freitag 2001, 2003; Freitag & Benz 2002) characterize capture as the point at which the gravitational wave inspiral timescale becomes comparable to the two-body scattering timescale. Equation (25) can be easily implemented in this context in place of the usual Peters & Mathews timescale (eq. [16]). More recently, Hopman & Alexander (2005) used Monte Carlo simulations to study the capture problem but allowed for diffusion by two-body scattering after gravitational wave emission had become important. They found that while the standard criterion, $\tau_{\rm gw} = (1-e)\tau_{\rm rlx}$, is a reasonable approximation, there was a significant effect from scattering after this point, with many stars being perturbed onto plunge orbits rather than capture orbits. However, once $\tau_{\rm gw} \lesssim 0.01(1-e)\tau_{\rm rlx}$, this effect was unimportant. At this point, the orbits are still in general extremely eccentric, and so the parabolic flux equations (13)–(15) and inspiral timescale (eq. [21]) are valid and improve significantly over Peters & Mathews. Thus, the improvements presented here could also be implemented easily in this type of diffusion calculation. In the future, we hope that the results in this paper will be usefully implemented in existing stellar cluster simulation codes to investigate what effect a more careful treatment of the gravitational radiation emission can have on capture rates.

The results presented here are strictly valid only for parabolic orbits but perform well for any orbit with sufficiently high eccentricity ($e \gtrsim 0.9$). We expect that in the capture problem, all orbits of interest will be highly eccentric. However, there are other astrophysically interesting scenarios in which inspiraling objects will begin on orbits with moderate or zero eccentricity. These include the formation of stars in an accretion disk around a black hole (Levin 2003; Goodman & Tan 2003), or the capture of stars by stripping of binaries in three-body encounters (Miller et al. 2005). In § 4 we described a simple trick that can be used to improve the accuracy of the Peters & Mathews approximation to the gravitational radiation fluxes for orbits of moderate eccentricity. Simply by using a different parameterization of the orbit and evaluating the usual flux expression for those parameters, significantly more accurate results can be obtained (Gair et al. 2005). The asymptotic approximation to the timescale in equation (21) is no longer accurate when the initial eccentricity is moderate. However, capture is usually not the interesting question in astrophysical scenarios where this occurs, since the stars have already been brought onto close orbits by other mechanisms and so it will not usually be necessary to evaluate the capture criterion $\tau_{\rm gw} < (1-e)\tau_{\rm rlx}$. If an inspiral timescale is required to determine the subsequent evolution, or parameter distribution of *LISA* sources, this may be computed by integrating the flux expressions along the inspiral trajectory. An important caveat is that the moderate eccentricity results quoted in § 4 do not approach the parabolic results (eqs. [13]–[15]) in the limit $e \to 1$, except in the weak field, $r_p \to \infty$. This is simply because the parabolic results are based on accurate perturbative calculations, while the results in § 4 are approximations. For this reason, it would be unwise to combine both approaches in any single calculation. However, generally speaking the astrophysical situations in which the parabolic results are applicable are quite distinct from those in which the moderate eccentricity approximations are required. If it is necessary to follow an inspiral from capture right up to plunge, a scheme should interpolate appropriately between the parabolic expression (eqs. [13]–[15]) and either the moderate eccentricity expressions quoted in

§ 4 or other schemes for evolving moderate eccentricity EMRIs (e.g., Barack & Cutler 2004; Gair & Glampedakis 2005).

The flux expressions (eqs. [13]–[15]) scale linearly with the mass ratio, m/M. This follows from the assumption of an extreme mass ratio, $m/M \ll 1$. As the mass ratio is increased, the approximations used here break down in various regimes. For highly eccentric orbits, the assumption that the gravitational wave emission can be averaged over the orbit no longer holds, and it is necessary to account for the fact that the emission occurs in short bursts near periapse. This was discussed at the end of § 3, and it can be accounted for in a reasonably simple way. A further consequence of increasing mass ratio is the failure of the adiabatic approximation. The energy and angular momentum fluxes are computed under the assumption that the source orbit is a geodesic of the spacetime. This is a reasonable assumption, provided that the timescale over which the orbital parameters change appreciably due to gravitational wave emission is long compared to the orbital timescale. This assumption breaks down if the mass ratio is too high or for orbits that lie close to the separatrix (for which the energy and angular momentum losses diverge). Roughly speaking, the adiabatic approximation breaks down when the change in eccentricity/periapse on a single encounter with the black hole is a significant fraction of the orbital eccentricity/periapse, but typically this only occurs close to plunge. The other problem at high mass ratio is the breakdown of the perturbative approach—equations (13)–(15) are based on a fit to calculations that have been carried out to leading order in the mass ratio. As the mass ratio becomes moderate, this is no longer sufficiently accurate. Broadly speaking, our results should apply to mass ratios less than $\sim 10^{-2}$ to 10^{-1}.

The results in this paper apply to orbits in the Schwarzschild spacetime, while theoretical models (Volonteri et al. 2005) and some observational evidence (Miniutti et al. 2004; Fabian et al. 2005) indicate that most astrophysical black holes will have significant spins. While some perturbative results are available that compute the radiation from orbits around spinning black holes (Poisson 2004), there is not yet sufficiently generic data available from state-of-the-art computations to fit for that situation. However, the arguments that led to the construction of the fitting function that performs so well in this case also apply when the central black hole has spin. Once a sufficient quantity of data is available, it should be possible to construct a fit of similar form, although it will be more complicated, as the fit will depend on three parameters—the black hole spin, the radius of the periapse, and the inclination of the orbit. For more generic applicability, eccentricity can also be included as a fourth parameter, although again this can only be done once perturbative calculations for generic orbits have been completed.

We thank Marc Freitag for useful discussions and comments on the manuscript. S. L. L. and J. R. G. thank the Aspen Centre for Physics for hospitality while the manuscript was being finished. This work was supported in part by NASA grants NAG5-12834 (J. R. G., D. J. K.) and NAG5-10707 (J. R. G.) and by St. Catharine's College, Cambridge (J. R. G.). S. L. L. acknowledges support at Penn State from the Center for Gravitational Wave Physics, funded by the NSF under cooperative agreement PHY 01-14375, as well as support from Caltech under *LISA* contract number PO 1217163.

REFERENCES

Barack, L., & Cutler, C. 2004, Phys. Rev. D, 69, 082005
Cutler, C., Kennefick, D., & Poisson, E. 1994, Phys. Rev. D, 50, 3816
Fabian, A. C., Miniutti, G., Iwasawa, K., & Ross, R. R. 2005, MNRAS, 361, 795
Freitag, M. 2001, Classical Quantum Gravity, 18, 4033
———. 2003, ApJ, 583, L21
Freitag, M., & Benz, W. 2002, A&A, 394, 345
Gair, J. R., Barack, L., Creighton, T., Cutler, C., Larson, S. L., Phinney, E. S., & Vallisneri, M. 2004, Classical Quantum Gravity, 21, 1595
Gair, J. R., & Glampedakis, K. 2005, Phys. Rev. D, submitted (gr-qc/0510129)
Gair, J. R., Kennefick, D., & Larson, S. 2005, Phys. Rev. D, 72, 084009
Goodman, J., & Tan, J. C. 2003, ApJ, 608, 108
Hils, D., & Bender, P. L. 1995, ApJ, 445, L7
Hopman, C., & Alexander, T. 2005, ApJ, 629, 362
Ivanov, P. B. 2002, MNRAS, 336, 373
Levin, Y. 2003, preprint (astro-ph/0307084)
Martel, K. 2004, Phys. Rev. D, 69, 044025
Miller, M. C., Freitag, M., Hamilton, D. P., & Lauburg, V. M. 2005, ApJ, 631, L117
Miniutti, G., Fabian, A. C., & Miller, J. 2004, MNRAS, 351, 466
Peters, P. C. 1964, Phys. Rev., 136, 1224
Peters, P. C., & Mathews, J. 1963, Phys. Rev., **131**, 435
Poisson, E. 2004, Living Rev. Relativity, 7, 6, http://www.livingreviews.org/lrr-2004-6 (accessed 2005 June 17)
Ruffini, R., & Sasaki, M. 1981, Prog. Theor. Phys., 66, 1627
Sigurdsson, S., & Rees, M. 1997, MNRAS, 284, 318
Volonteri, M., Madau, P., Quartet, E., & Rees, M. 2005, ApJ, 620, 69